Nonlinear wind turbine control under wind speed variation and voltage dips

Abdelhaq.Amar bensaber[1]
abs.abdelhak@gmail.com

Mustapha Benghanem[1]
mbenghanem69@yahoo.fr

Abdelmadjid.Guerouad[1]
a.guerouad@yahoo.com

Mohammed Amar bensaber[2]
m.amarbensaber@esi-sba.dz

[1]AVCIS Laboratory - Oran University of Science and Technology - Mohamed Boudiaf –
[2]School of Computer Science 08 May 1945 Sidi Bel Abbès

Abstract— *Doubly Fed Induction Generator is an attractive solution in variable wind turbines[1, 2] because of its features like lessening losses, minimum cost, an improved efficiency and power control capabilities[2]. Traditionally the control is based on PI controller which is advisable just for linear systems. However, wind turbines components work as nonlinear systems where electromechanical parameters change frequently [3], thus ,a SOMC is proposed and then a modest function to smooth control signal is introduced which will improve power fineness, minimize the chattering and ameliorate respond time, deal with grid requirements. Matlab tests are introduced and compared.*

Keywords-component; SMC, DFIG, Active and Reactive Power control , MPPT, Sliding mode control. TAN, SOSM.

I. Introduction

Concerns over the environmental impacts and scarcity of fossil fuels have led to move towards the clean and inexhaustible power. Compared with other clean energies, wind power has been proved as one acknowledged potential source of energy, like it cost efficiency and reliability [4, 5]. Thus, those factors became important topics in industry and research [6, 7].Control strategies are necessary to attain maximum performance. The DFIG WTs has been an attractive choice [8, 9] because of to the independent power control plus it ability to deal with variable speed due to control of back-to-back converter scheme[10, 11], reduced mechanical stresses[2], recompense for power pulsations and torque [12] and improve power quality[2] ,the major feature of proposed generator is that the power converter is sized between "20–30%" of entire power which means the cost is reduced[13], still the generator respond to voltage disturbances is critical, as expressed in [2, 14] , ,to protect and remain connected to the network even with faults it is required to control the rotor converter. [2, 14-16], the control schemes are established with the vector control with the classical controller, but this controller can provide favorable performance restrictive under ideal voltage conditions. Furthermore, disturbances and parameter variations will leave us with imperfect performance. Therefore, papers have offered many control strategies for DFIG like Sliding Mode Control, smart control or adaptive algorithms [1, 17, 18], HOSMC [6, 15, 16, 19, 20]. SMC, despite robust, it suffers two main deficiencies. First, chattering phenomenon which produced from the high-frequency switching that damage the performance and excites high frequency oscillations [21, 22]. To overthrown these problems, many authors proposed to modify the SMC law [15, 23-25].

In this present paper, SMC is suggested to regulate the power swapped between the generator and the grid , to overcome it drawbacks many of methods were proposed like approximating the sign function by a high gain saturation function [26] , we decide to use SOMC because it has several features like:

- Robustness [27, 28].
- subtraction of mechanical stresses and chattering[28].
- Easy to implement[28].

We proposed an improvement to the 2SMC by adjusting the discontinuous control signal toward sliding surface, PI, SMC and 2SMC controllers are compared, we aim to see how SOMC can improve performances. This article arranged as follows; turbine model and the MPPT are given in the second section. In part III, DFIG mathematical model is introduced. Section IV introduces DFIG Vector Control. In section V SOMC is proposed. At last, matlab results are given and debated.

II. MODEL OF THE TURBINE:

The power contained in the form of kinetic energy at a speed V_v, surface A_1, is expressed by

$$P_v = \frac{1}{2}\rho A_1 V_v^3 \tag{1}$$

Where ρ is the air density, but the wind turbine is can regain only a part of that power:

$$P_v = \frac{1}{2}\rho\pi R^2 V_v^3 C_p \tag{2}$$

Where: R is the radius; Cp is power coefficient [23], this coefficient is a related with the wind and wind turbine rotation pace and the pitch angle.

The speed ratio λ introduced by:

$$\lambda = \frac{R\Omega_t}{V_v} \qquad (3)$$

Where R is the blades length, Ω_t is the rotor angular speed. The theoretical extreme rate of C_p is given by the Betz limit

$$C_{p\_theo\_max} = 0,593 = 59,3\%$$

The torque and power coefficient C_p is represented in function of tip step ratio (λ) and the pitch angle (β) as fellow:

$$C_p = C_1(\frac{C_2}{\lambda_i} - C_3\beta - C_4\beta^{C_5} - C_6)(e^{C_7/\lambda_i}) \qquad (4)$$

$$\lambda_i = \frac{1}{\lambda + C_8} \qquad (5)$$

The slow shaft mechanical torque C_t is expressed by:

$$C_t = \frac{P_t}{\Omega_t} = \frac{\pi}{2\lambda}\rho R^3 v^2 C_p \qquad (6)$$

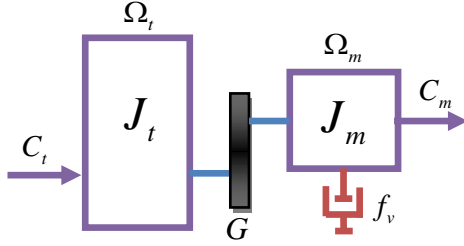A. *Mechanical System:* The mechanical model will be illustrated in Figure 1

Figure 1 : Mechanical model

Where: J_t: the turbine inertia, while J_m : generator inertia, G is the gearbox ratio. The generator speed and the fast shaft torque are given in:

$$\Omega_m = G\Omega_t \quad (7) \qquad C_m = C_t/G \quad (8)$$

Next,

$$C_m - C_{em} = \left(\frac{J_t}{G^2} + J_m\right)\frac{d\Omega_m}{dt} + f_v\Omega_m \quad (9)$$

B. *Maximum Power Tracking MPPT*

Aiming to extract the supreme power is the fundamental objective of the speed control. Many methods are used to ensure that [29, 30]. Direct speed controller (DSC) is presented in fig 2, its concept is founded on generating the optimal turbine speed for various wind speed value, and use it as speed reference. Next, with the help of a regulator the turbine rotational speed is controlled and the mechanical power aimed to be maximal for each operating point; the reference rotational speed is defined by:

$$\Omega_t^* = \left(\lambda_{opt}v\right)/R \quad (10) \quad \text{Thus,} \quad \Omega_m^* = G\Omega_t^* \qquad (11)$$

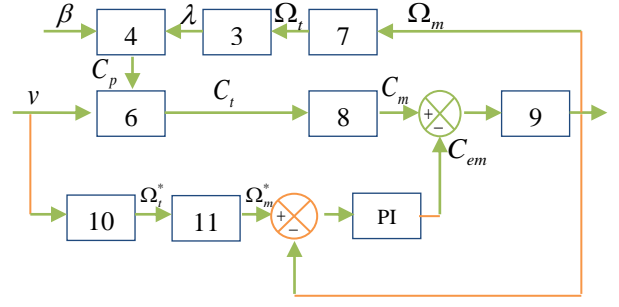
Figure 2 :Direct speed control.

We obtain the active power reference by the following equation:

$$P_{s\_ref} = C_{cem\_ref}\Omega_m \qquad (12)$$

III. MATHEMATICAL MODEL OF DFIG:

We have chosen to use the double-fed induction generator because with the help of the bidirectional converter in the rotor it is possible to work in both sub-synchronous and super-synchronous. The electrical model of the machine obtained using Park transformation is given by the following equations [23, 30, 31]:

Stator, rotor voltages: Eqts (13-16)

$$V_{qs} = R_s I_{qs} + \frac{d\phi_{qs}}{dt} - \omega_s\phi_{ds} \; ; \; V_{ds} = R_s I_{ds} + \frac{d\phi_{ds}}{dt} - \omega_s\phi_{qs}$$

$$V_{dr} = R_r I_{dr} + \frac{d\phi_{dr}}{dt} - \omega\phi_{qr} \; ; \; V_{qr} = R_r I_{qr} + \frac{d\phi_{qr}}{dt} - \omega\phi_{dr}$$

Where: $$\omega = \omega_s - \omega_m \qquad (17)$$

Stator, rotor fluxes:

$$\phi_{ds} = L_s I_{ds} + MI_{dr} \qquad (18) \qquad \phi_{qs} = L_s I_{qs} + MI_{qr} \qquad (19)$$

$$\phi_{dr} = L_r I_{dr} + MI_{ds} \qquad (20) \qquad \phi_{qr} = L_r I_{qr} + MI_{qs} \qquad (21)$$

The electromagnetic torque is:

$$C_{em} = P\left(\phi_{ds}I_{qs} - \phi_{qr}I_{ds}\right) = PM\left(I_{dr}I_{qs} - I_{qr}I_{ds}\right) \qquad (22)$$

The motion equation is:

$$C_{em} - C_r = J\frac{d}{dt}\Omega_m + f_v\Omega_m \quad (23) \quad J = \frac{J_{turbine}}{G^2} + J_g \quad (24)$$

Where: the load torque is C_r, J is the total inertia, mechanical speed is Ω_r.

IV. The DFIG Vector Control:

In this section, the application of vector control DFIG is to achieve a decoupling between the quantities generating torque and flux. For this, we adjust the flux by (I_{ds} or I_{dr}), and torque by (I_{qs} or I_{qr}). Thus, the dynamics of DFIG will be reduced to that of a DC machine. This method can be outlined as shown in Fig 3.
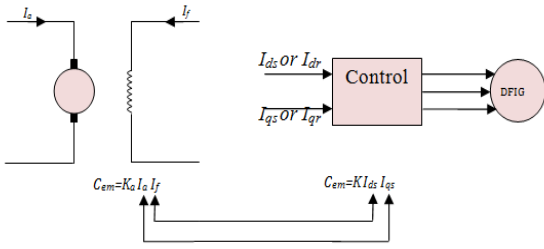
Figure 3 : Analogy between the vector control of DFIG and the control of a DC machine.

The doubly fed induction generator model can be described by the next equations in the synchronous frame whose axis d is aligned with the stator flux vector as shown in fig. 4, ($\phi_{ds} = \phi_{qs}$) and ($\phi_{qs} = 0$) [7, 23, 30, 32]. By neglect stator resistances voltage will be:

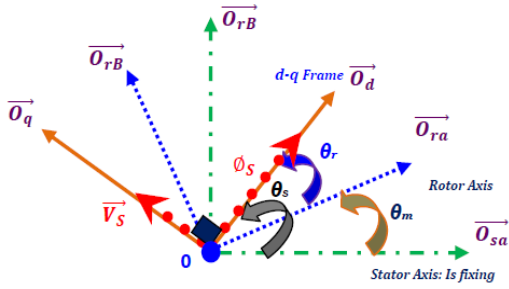$$V_{ds} = 0 \text{ and } V_{qs} = V_s = \omega_s \phi_s \quad (25)$$

Figure 4 : Stator and rotor flux vectors in the synchronous d-q Frame.

We driver to an uncoupled power control; where, I_{dr} controls the active power, and the reactive power is controlled by the direct component I_{ds} [33]as shown in fig. 5:

$$P_s = -V_s \frac{M}{L_s} I_{qr} \quad (26)$$

$$Q_s = \left(\frac{\phi_s V_s}{L_s} - \frac{M}{L_s} V_s I_{dr} \right) = \left(\frac{V_s^2}{\omega_s L_s} - \frac{M}{L_s} V_s I_{dr} \right) \quad (27)$$

The equations of the voltages according to the rotor currents are shown below (fig. 5):

$$V_{dr} = R_r I_{dr} + L_r \sigma \frac{dI_{dr}}{dt} - L_r \sigma \omega I_{qr} \quad (28)$$

$$V_{qr} = R_r I_{qr} + L_r \sigma \frac{dI_{qr}}{dt} - L_r \sigma \omega I_{dr} + \frac{M}{L_s} \omega \phi_s \quad (29)$$

With: $\quad \sigma = \left(1 - M^2 \right) / L_s L_r \quad (30)$

Where: V_{dr}, V_{qr} are rotor voltage; R_r is the rotor resistances; L_r, L_s are the rotor inductances; M is mutual inductance; σ is leakage factor.
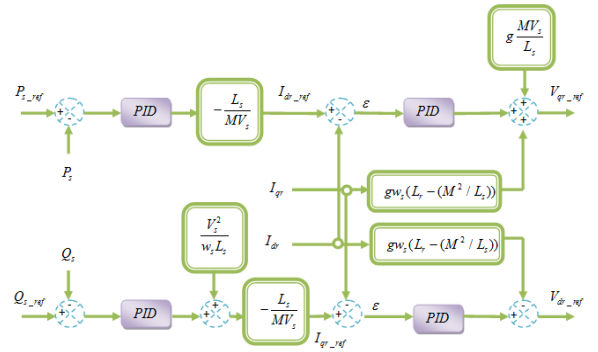

Figure 5 : Power Control.

V. The sliding mode control

The main advantage of this control is its simplicity and robustness in spite of uncertainties in the system and external disturbances and on the other hand it needs relatively less information about the system and also is insensitive to the parametrical changes of the system plus it doesn't need to the mathematical models accurately like classical controllers but needs to know the range of parameter changes for ensuring sustainability and condition satisfactory [15, 16, 19, 20]. The sliding mode control has three stages: Choice of surface, Convergence condition and Calculation of the control laws.

Second Order Sliding Mode Control

SMC is an interesting nonlinear method approach. Nevertheless, the biggest problem of this control is the chattering phenomenon which causes mischievous effects on the generator because of the discontinuous surveillance and that cause overheating and trigger unmodeled high frequency dynamics [34]. SOMC is an attractive solution [35] , it generalizes the sliding mode idea by going to a higher order time derivatives, which decrease chattering and avoid powerful mechanical efforts while maintaining advantages of the SMC [34, 35], such as robustness under uncertainties. Aiming at achieving satisfactory tracking performance for Ps and Qs, the switching functions given next are adopted

$$\begin{cases} S_P = e_P + c_P \int e_P dt \\ S_Q = e_Q + c_Q \int e_Q dt \end{cases} \quad (31)$$

The integral terms c_P sand c_Q are positive constant, are added for steady-state errors elimination [6, 34]. The voltage applied represented in the equation below:

$$\begin{cases} V_{dr} = V_{dreq} + V_{drn} \\ V_{qr} = V_{qreq} + V_{qrn} \end{cases} \quad (32)$$

The system in reach the sliding surface with the help of the switching control V_{drn} and V_{qrn} ; V_{qreq} and V_{dreq} are the equivalent control terms ,they make the system move along the sliding manifold and accelerate the response of the system while reducing the steady-state errors[36]. The equivalent

control terms are derived by letting $\dot{S}_P = \dot{S}_Q = 0$, the voltage to be applied to the rotor are expressed as (33)

$$\begin{cases} V_{qreq} = -\dfrac{L_s L_r \sigma}{MV_s}\left(\dot{P}_{s\_ref} + c_P\left(P_{s\_ref} - P_s\right)\right) + R_r I_{qr} - g w_s L_r \sigma I_{dr} - g\dfrac{MV_s}{L_s} \\[3mm] V_{dreq} = -\dfrac{L_s L_r \sigma}{MV_s}\left(\dot{Q}_{s\_ref} + c_P\left(Q_{s\_ref} - Q_s\right)\right) + R_r I_{dr} - g w_s L_r \sigma I_{qr} \end{cases}$$

Thus (34);

$$\begin{cases} V_{drn} = y_1 + B_1 |e_P|^{\frac{1}{2}} sign\left(e_Q\right) \qquad \dot{y}_1 = B_2 sign\left(e_Q\right) \\[3mm] V_{qrn} = y_2 - B_3 |e_P|^{\frac{1}{2}} sign\left(e_P\right) \qquad \dot{y}_2 = -B_4 sign\left(e_P\right) \end{cases}$$
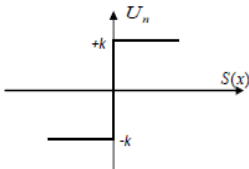
Where the constants B1, B2, B3 and B4

$$\begin{cases} B_1 \succ \dfrac{\Phi_2}{\sigma L_r} \qquad B_2^2 \geq \dfrac{4\Phi_1\left(B_1 + \Phi_1\right)}{\sigma^2 L_r^2\left(B_1 - \Phi_1\right)} \\[3mm] B_3 \succ p\dfrac{M}{\sigma L_r L_s}\Phi_1 \qquad B_4^2 \geq \dfrac{4\Phi_2\left(B_3 + \Phi_2\right)}{\sigma^2 L_r^2\left(B_3 - \Phi_2\right)} \\[3mm] \left|\dot{G}_1\right| \prec \Phi_1 \qquad \left|\dot{G}_2\right| \prec \Phi_2 \end{cases} \qquad (35)$$
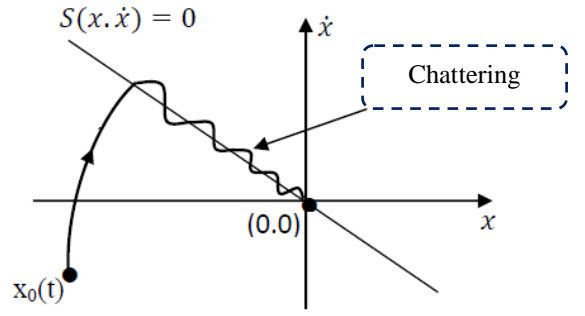
And (36),

$$\begin{cases} G_1 = \dot{P}_{s\_ref} + V_s\dfrac{M}{L_s L_r \sigma}\left(-R_r I_{qr} + g w_s L_r \sigma I_{dr} + g\dfrac{MV_s}{L_s}\right) \\[3mm] G_2 = \dot{Q}_{s\_ref} + V_s\dfrac{M}{L_s L_r \sigma}\left(-R_r I_{dr} + g w_s L_r \sigma I_{qr}\right) \end{cases}$$

The function sign is defined as:

$$sign(\phi) = \begin{cases} 1 \ , \ if \ \ \phi \succ 0 \\ 0 \ , \ if \ \ \phi = 0 \\ 1 \ , \ if \ \ \phi \prec 0 \end{cases}$$

However, the latter generates on the sliding surface, a phenomenon called chattering, which is generally undesirable because it adds to the spectrum control high frequency components.

Chattering Phenomenon.

In Order to minimize the chattering we will change the sign function with hyperbolic tangent function which will smooth the control signal across the sliding surface, the function is shown in Figure 6 and it's defined by:

$$U_n = K\dfrac{S(x)}{\left|S(x)\right| + \delta} + \eta \qquad (44)$$

Thus,

$$\delta = \begin{cases} \delta_0 & if \ \left|S(x)\right| \geq \varepsilon \\[2mm] \delta_0 + \gamma\int S(x)dt & if \ \left|S(x)\right| \prec \varepsilon \end{cases} \qquad (45)$$

$$\eta = \begin{cases} 0 & if \ \left|S(x)\right| \geq \varepsilon \\[2mm] \xi\int S(x)dt & if \ \left|S(x)\right| \prec \varepsilon \end{cases} \qquad (46)$$

Where: $\delta, \eta, \xi, \varepsilon, \gamma$ are positive constants.
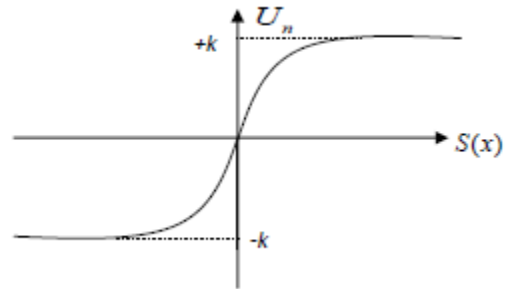

Figure 6 : hyperbolic tangent function.

VI.   SIMULATION RESULTS

In this section, simulation tests have been performed with the help of Matlab. A performance comparison with two different linear and nonlinear controllers "PI, SMC and 2-SMC" will be introduced and discussed
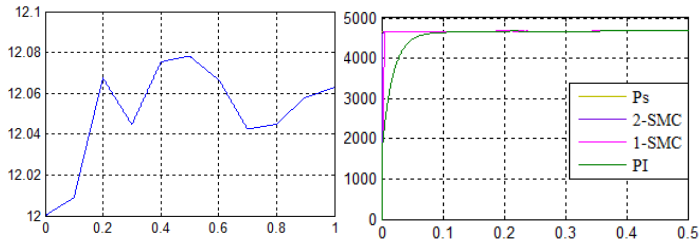
Wind speed shown in Fig (7) in order evaluates the designed control.
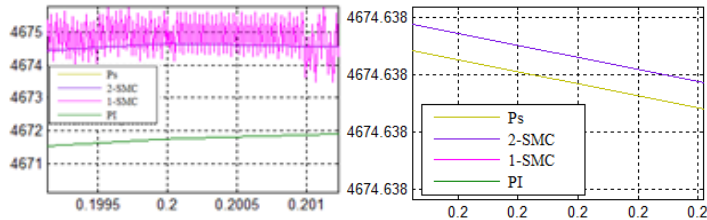

Figure 7 : Wind speed

Figure 8 : Stator Active power Ps

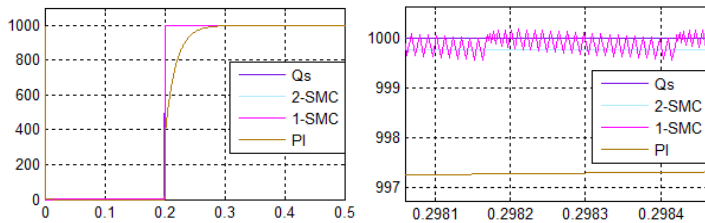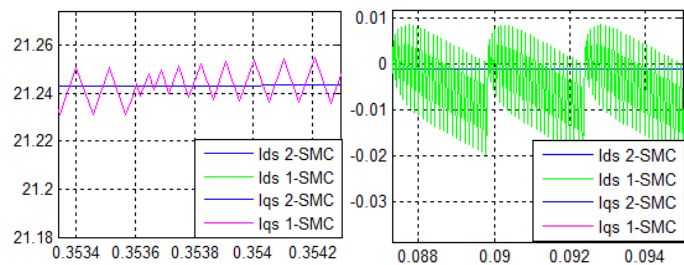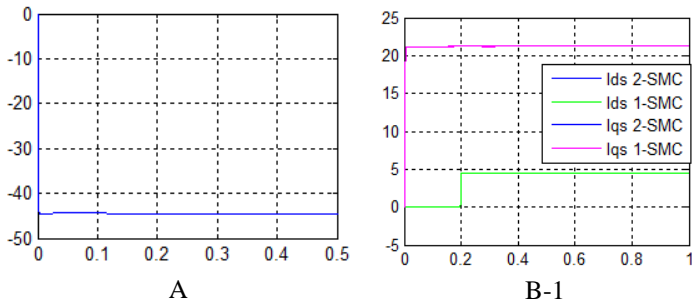Figure 9 : Reactive Active power Qs

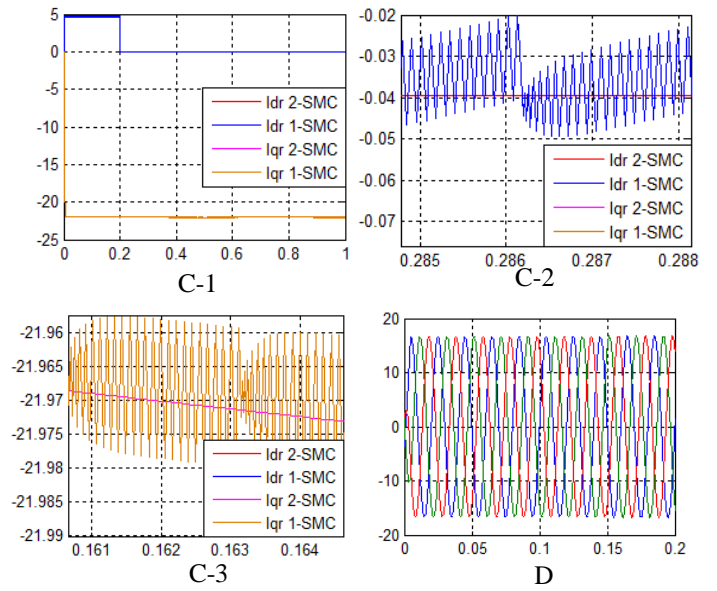

A

B-1

B-2

B-3

C-1

C-2

C-3

D

Figure 10: a- Electromagnatique couple b- Rotor current components

Fig 8 and 9 represent the stator active and reactive powers and its reference profiles using PI and SMC, we can notice that the dynamic response under the PI control is much slower than SMC control while SMC tracks almost perfectly their references .However the first order sliding mode controller includes an appearance of perturbations which presented through the chattering phenomenon after zooming, we can see clearly that the 2SMC with the tan function could smooth the control signals and that caused an elimination of chattering phenomenon. This outcome tends to guarantee stability and the power quality even when there is a change in wind speed. The electromagnetic torque represented in Fig (10-A) is negative due to the generator operation. We can notice a great decoupling among the rotor and stator current components is obtained as shown in fig 10-C-D which guarantee a decoupled powers control .Our system is examined under a stator voltage drop between 1.5s and 1.6 s, as shown in Fig. 11; a good decoupling between stator components is obtained as shown in fig 12, which guarantee a decoupled control of powers.
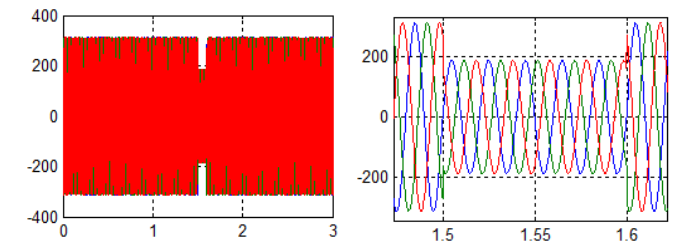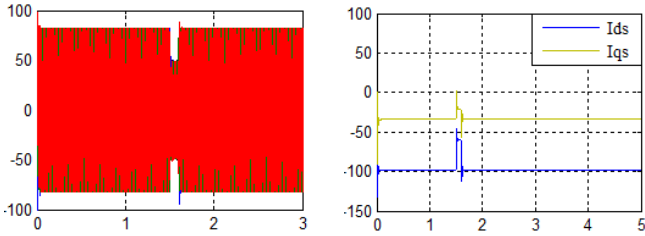

Figure 11: stator voltage

Figure 12: stator courant

VII. CONCLUSION

In this paper, we have presented a complete system to produce electrical energy with a doubly-fed induction generator in wind turbine is presented and controlled using the sliding mode control than a solution to improve the control was proposed, simulation results show that the proposed controller provides a notable efficiency, since it permits to track the optimum power quickly despite the speed wind changing. On the other hand, the stator power quantities provided show smooth waveforms, with good tracking indices. Consequently, undesirable mechanical stresses and the chattering phenomena are avoided

APPENDIX

The generator's parameters are presented below: Rs = 1.2Ω, Rr = 1.8Ω, Ls = 0.1554H, Lr= 1.558 H, M = 0.15, Vs=380 V/220V; P= 2, Fr=0.0027N.s/rad, f=50Hz; J=0.042 kg.m2, Aerodynamic coefficients C1=0.5, C2=116, C3=0.4, C4=0, C5=5, C6=21, controller parameter:

$$K_p = \frac{t_r}{L_r}, \ K_i = \frac{K_p R_r}{L_r \sigma}, \ K_{p\_Ir} = \frac{L_s L_r \sigma}{M V_s t_r},$$

$$K_{i\_Ir} = \frac{K_{p\_Ir} R_r}{L_r \sigma}$$

REFERENCES

[1] A.M. Kassem, K.M. Hasaneen, A.M. Yousef, Dynamic modeling and robust power control of DFIG driven by wind turbine at infinite grid, International Journal of Electrical Power & Energy Systems 44(1) (2013) 375-382.

[2] N.H. Saad, A.A. Sattar, A.E.-A.M. Mansour, Low voltage ride through of doubly-fed induction generator connected to the grid using sliding mode control strategy, Renewable Energy 80 (2015) 583-594.

[3] D.H. Phan, S. Huang, Super-Twisting Sliding Mode Control Design for Cascaded Control System of PMSG Wind Turbine, Journal of Power Electronics 15(5) (2015) 1358-1366.

[4] H.T. Jadhav, R. Roy, A comprehensive review on the grid integration of doubly fed induction generator, International Journal of Electrical Power & Energy Systems 49 (2013) 8-18.

[5] S. Abdeddaim, A. Betka, Optimal tracking and robust power control of the DFIG wind turbine, International Journal of Electrical Power & Energy Systems 49 (2013) 234-242.

[6] E.C. López, J. Persson, High-Order Models of Doubly Fed Induction Generators, Wind Power in Power Systems, John Wiley & Sons, Ltd2012, pp. 849-864.

[7] M. Yamamoto, O. Motoyoshi, Active and reactive power control of doubly-fed wound rotor induction generator, 21st Annual IEEE Conference on Power Electronics Specialists, 1990, pp. 455-460.

[8] H. Li, Z. Chen, Overview of different wind generator systems and their comparisons, IET Renewable Power Generation, Institution of Engineering and Technology, 2008, pp. 123-138.

[9] A. Hansen, P. Sø rensen, F. Blaabjerg, F. Iov, {Centralised power control of wind farm with doubly fed induction generators}, Renewable Energy 31(7) (2006) 935-951.

[10] N.D. Caliao, Dynamic modelling and control of fully rated converter wind turbines, Renewable Energy 36(8) (2011) 2287-2297.

[11] F.E.V. Taveiros, L.S. Barros, F.B. Costa, Back-to-back converter state-feedback control of DFIG (doubly-fed induction generator)-based wind turbines, Energy 89 (2015) 896-906.

[12] W. Qiao, Dynamic modeling and control of doubly fed induction generators driven by wind turbines, 2009 IEEE/PES Power Systems Conference and Exposition, 2009, pp. 1-8.

[13] T. Ahmed, K. Nishida, M. Nakaoka, A Novel Stand-Alone Induction Generator System for AC and DC Power Applications, IEEE Transactions on Industry Applications 43(6) (2007) 1465-1474.

[14] J. Lopez, P. Sanchis, X. Roboam, L. Marroyo, Dynamic Behavior of the Doubly Fed Induction Generator During Three-Phase Voltage Dips, IEEE Transactions on Energy Conversion 22(3) (2007) 709-717.

[15] J.B. Alaya, A. Khedher, M.F. Mimouni, Nonlinear vector control strategy applied to a variable speed DFIG generation system, Eighth International Multi-Conference on Systems, Signals & Devices, 2011, pp. 1-8.

[16] Y. Shtessel, C. Edwards, L. Fridman, A. Levant, Sliding Mode Control and Observation, Springer New York2013.

[17] Z. Song, T. Shi, C. Xia, W. Chen, A novel adaptive control scheme for dynamic performance improvement of DFIG-Based wind turbines, Energy 38(1) (2012) 104-117.

[18] D. Zhi, L. Xu, J.A. Morrow, Improved direct power control of doubly-fed induction generator based wind energy generation system, 2007, pp. 436-441.

[19] J.J.E. Slotine, W. Li, Applied Nonlinear Control, Prentice-Hall1991.

[20] B. Yang, L. Jiang, L. Wang, W. Yao, Q.H. Wu, Nonlinear maximum power point tracking control and modal analysis of DFIG based wind turbine, International Journal of Electrical Power & Energy Systems 74 (2016) 429-436.

[21] M.J. Morshed, A. Fekih, A new fault ride-through control for DFIG-based wind energy systems, Electric Power Systems Research 146 (2017) 258-269.

[22] J.G. Njiri, D. Söffker, State-of-the-art in wind turbine control: Trends and challenges, Renewable and Sustainable Energy Reviews 60 (2016) 377-393.

[23] G. Abad, J. López, M.A. Rodríguez, L. Marroyo, G. Iwanski, Direct Control of the Doubly Fed Induction Machine, Doubly Fed Induction Machine, John Wiley & Sons, Inc.2011, pp. 363-477.

[24] A. Luna, F.K.A. Lima, P. Rodriguez, E.H. Watanabe, R. Teodorescu, Comparison of power control strategies for DFIG wind turbines, 2008 34th Annual Conference of IEEE Industrial Electronics, 2008, pp. 2131-2136.

[25] M. Benkahla, R. Taleb, Z. Boudjema, Comparative Study of Robust Control Strategies for a Dfig-Based Wind Turbine, INTERNATIONAL JOURNAL OF ADVANCED COMPUTER SCIENCE AND APPLICATIONS 7(2) (2016) 455-462.

[26] S. Li, T.A. Haskew, R.P. Swatloski, W. Gathings, Optimal and Direct-Current Vector Control of Direct-Driven PMSG Wind Turbines, IEEE Transactions on Power Electronics 27(5) (2012) 2325-2337.

[27] E. Bounadja, A. Djahbar, R. Taleb, Z. Boudjema, A new adjustable gains for second order sliding mode control of saturated DFIG-based wind turbine, AIP Conference Proceedings 1814(1) (2017) 020009.

[28] C. Evangelista, P. Puleston, F. Valenciaga, Wind turbine efficiency optimization. Comparative study of controllers based on second order sliding modes, international journal of hydrogen energy 35(11) (2010) 5934-5939.

[29] S.E. Aimani, Modélisation des différentes technologies d'éoliennes intégrées dans un réseau de moyenne tension, 2004.

[30] F. Poitiers, ETUDE ET COMMANDE DE GENERATRICES ASYNCHRONES POUR L'UTILISATION DE L'ENERGIE EOLIENNE
 - Machine asynchrone à cage autonome
 - Machine asynchrone à double alimentation reliée au réseau, Université de Nantes, 2003.

[31] X. Lie, P. Cartwright, Direct active and reactive power control of DFIG for wind energy generation, IEEE Transactions on Energy Conversion 21(3) (2006) 750-758.

[32] M. Rahimi, M. Parniani, Dynamic behavior analysis of doubly-fed induction generator wind turbines – The influence of rotor and speed controller parameters, International Journal of Electrical Power & Energy Systems 32(5) (2010) 464-477.

[33] K. Jemmli, M. Jemli, M. Gossa, M. Boussak, Power flow control and VAR compensation in a doubly fed induction generator, International Journal

of Sciences and Techniques of Automatic control & computer engineering, Special issue CEM (2008) 548-565.

[34] F. Valenciaga, P.F. Puleston, High-Order Sliding Control for a Wind Energy Conversion System Based on a Permanent Magnet Synchronous Generator, IEEE Transactions on Energy Conversion 23(3) (2008) 860-867.

[35] W. Wen-Jieh, C. Jenn-Yih, Passivity-based sliding mode position control for induction motor drives, IEEE Transactions on Energy Conversion 20(2) (2005) 316-321.

[36] X. Zhu, S. Liu, Y. Wang, Second-order sliding-mode control of DFIG-based wind turbines, (2014).